Deconvolution in the presence of stratigraphic filtering

Verónica L. Martínez *, Dr. Mauricio D. Sacchi, University of Alberta, Edmonton, Canada.

Abstract

Seismic exploration is a powerful tool for imaging the subsurface of the Earth. There are cases, however, where although sonic logs exhibit significant velocity stratification, seismic processing is unable to obtain a well defined image of the reflectors. The case of non-resolvable layers like coal seams or carbonates that present strong impedance contrast with the background are a common example.

Deconvolution permits us to enhance data resolution. However, in the presence of a cyclic reflectivity this task becomes quite difficult due to the interference between the primary signal and many short-period multiples coming from that cyclic pattern. Then the multiple overlies the primary and modifies it by this superposition. Since we are dealing with multiples beyond seismic resolution, NMO (normal moveout correction) and deconvolution fail to isolate the primary arrival.

Since real data present a mixture of transitional and cyclic reflectivities, the wavelet will be distorted as it travels through the earth, changing its phase and amplitude spectrum, being this effect more critical under the presence of a cyclic pattern. Windowed deconvolution seems to be the best way to deal with non-stationarity. Identifying different windows that should be compensated for the lack of frequency content in order to recover a wavelet consistent within the complete seismogram.

This work is intended to propose a processing sequence that helps to compensate for that loss of frequency and therefore achieve a better image of the subsurface by improving the deconvolution processing step.

Cyclic and transitional reflectivity series

The subsurface can be characterized by changes due to different acoustic properties of successive layers. These changes are related to the reflectivity of the subsurface. One can distinguish two extreme types of reflectivity, *cyclic* and *transitional*.

These types of reflectivity are associated with two extreme cases of layering. Cyclic layering is a pattern of thin layers that alternate high and low velocity materials. Thin layers in this context are defined as those whose thickness is beyond the seismic resolution. This is to say, layers with thickness less than about $\lambda/8$, where λ is the (predominant) wavelength computed using the velocity of the layer. In the presence of noise the threshold of resolution is forced to thicker layers; less than $\lambda/4$ (Widess, 1973).

Transitional layering would imply steady gradations of velocity within thick layers (O'Doherty and Anstey, 1971}. In terms of reflectivity it is found that for the former type, the reflection coefficients tend to be big and with alternating sign, due to the significant contrast of velocities at every interface. On the other hand, for the latter type, reflection coefficients are small since the contrasts on the layer properties are not so drastic.

Real data, in many cases it is a mixture of these two types of layering. A clear example is shown by the reflectivity series corresponding to well data from the Rosebud area in the Western Canadian Sedimentary Basin (WCB), Alberta, Canada. The cyclic pattern, in this case, is given by the presence of coal seams. These are thin layers of 1 to 10 m thickness with velocity and density half of the background in packages of 20 to 30 m. An example of these data is shown in figure (1) where sections of transitional and cyclic layering are identified.
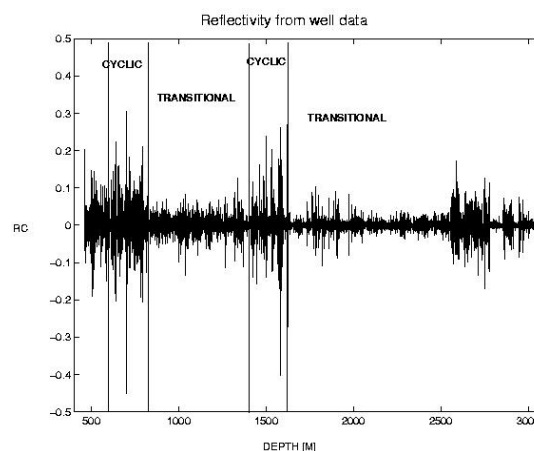

Figure 1: Reflectivity series corresponding to a well in the Western Canadian Basin.

Stratigraphic filtering

Once that the concept of cyclic and transitional reflectivitites where presented, let us now focus on the study of the Earth impulse response when the Earth consists of a vertically stratified succession of layers. There are two main factors to consider. First, the interface transmission losses and secondly multiple reflection effects. These effects are critical in the case of cyclic impedance stratification. Interference between primary and short path multiples is the key point to understand the frequency attenuation of the transmitted signal.

The term *stratigraphic filtering* or *layering filtering* is used in the literature for the shaping of transmitted waves by superposition of multiples reverberating in beds too thin to be resolved individually (Banik2 et al., 1985a). O'Doherty

and Anstey (1971) found an approximate relationship between the amplitude spectrum $T(\omega)$ of the transmitted pulse and the power spectrum $R(\omega)$ of the reflection coefficients series, given by

$$T(\omega)= e^{-R(\omega)\,\Delta t} \qquad\qquad (1)$$

where Δt is the traveltime of the directly transmitted wave.

The key concept to understand the idea of stratigraphic filtering is the interference between primary and short-period multiples. The qualifier ``short-period'' means the time difference between primary and first multiple is less than the width of the propagating wavelet. Thus the multiple does not show as a distinct arrival but rather, it overlies and modifies the primary by superposition. Then, as more and more multiples are superposed, the primary itself is decreased by transmission losses until the propagating wavelet is purely multiple energy.

It is this transformation from primary to superposition of multiples that may be conceived as a filter. Since the cause of this filtering is the presence of successive beds too fine to be resolved, the term ``stratigraphic filtering'' or ``layering filtering'' is appropriate. Studies on this subject indicate that the qualitative effects of stratigraphic filtering are preferential attenuation of high frequencies. The apparent attenuation in stratigraphic filtering is due to loss of coherence not absorption of energy (Banik et al., 1985b).

Schoenberg and Levin (1974) studied the apparent attenuation due to intrabed multiples and found that transmission losses attenuates amplitudes uniformly at all frequencies, while intrabed multiples tend to raise the amplitudes at the low-frequency end of the spectrum and lower those at the high frequency end. When the input pulse pass through a cyclic section, the transmitted signal appears broaden with a set of intrabed multiples following it.
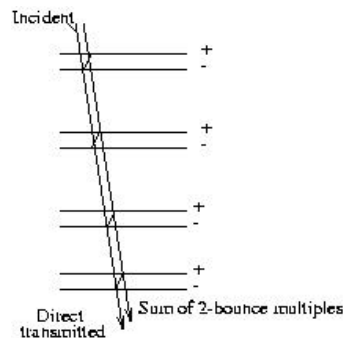

Figure 2: The cumulative effect of the multiple reflections for a sequence of thin unresolvable layers.

Deconvolution in the presence of stratigraphic filtering

So far, it was explained two different types of reflectivities, transitional and cyclic. Real log data are often composed of a mixture of these reflectivities. It was explained how the impulse response is distorted when a cyclic reflectivity is present. When a wave is traveling through such a profile it will suffer distortions, mainly in the amplitude spectrum. The main consequence will be the non-stationarity of the signal. The signal looses frequency content while is passing through what it is called *stratigraphic filter*. However, it is possible to design a filter that is able to compensate for most of this effect.

Deconvolution is a process that improves the temporal resolution of seismic data by compressing the basic seismic wavelet (Yilmaz,1987). However, in the presence of layering filtering, conventional deconvolution is not capable of recovering the ``right wavelet'' below the stratigraphic filter. It is clear that it is necessary to explore the data by windows and compensate somehow the effect due to this layering filter. This could be achieved by taking time windows above and below the stratigraphic filter from the stack seismogram $s_{above}(t)$ and $s_{below}(t)$. Then, we compute the amplitude spectrum above $A_{above}(\omega)$ and below $A_{below}(\omega)$ the transmission filter using the periodogram technique. Then, a transfer function can be computed by dividing these spectra in the frequency domain for the range of frequency of interest.

$$TRF(\omega) = \frac{A_{above}(\omega)}{A_{below}(\omega)} \quad , \qquad\qquad (2)$$

$TRF(\omega)$ being the amplitude spectrum of the filter to be applied to the window below the stratigraphic filter. Using the Hilbert transform H (Claerbout, 1976) it is possible to determine a minimum phase filter $trf_{min}(t)$ for the given amplitude spectrum $TRF(\omega)$,

$$trf_{min}(t) = H[TRF(\omega)] . \qquad\qquad (3)$$

Once the transfer filter $trf_{min}(t)$ was computed, it can be convolved with the data below the stratigraphic filter, $s_{below}(t)$

$$s_{below}^{filtered}(t) = s_{below}(t) * trf_{min}(t) . \qquad\qquad (4)$$

Now, applying conventional deconvolution to the windows above and below should yield to approximate the same wavelet. This approach could be a simple way to compensate the problems of the non-stationarity of the wavelet due to the stratigraphic filtering. The main difficulty on this technique is the criteria for choosing the length and position of the windows to isolate the wavelet below and above the sequence generating the stratigraphic filtering.

Examples

This synthetic example is generated using a model illustrated in figure (3). Coal layers are characterized with low density and velocity (ρ_{coal} = 1.7 g/cc and v_{coal} = 2400 m/s), while the background has velocity and density almost twice the former ones ($\rho_{background}$=2.2 g/cc and $v_{background}$ = 4200 m/s) for the stratigrafic filter.

The package of layers within the transmission filter were designed taking into account the condition of non-resolvable layers. That is to say, the thickness is less than about $\lambda/8$, where λ is the (predominant) wavelength computed using the velocity of the layer. As a source for

the propagation of waves it was used a 50 Hz Ricker wavelet, the sampling interval chosen is 0.002 sec.

First, we compute the amplitude spectrum of the O'Doherty and Anstey theoretical transmission filter generated by the present reflectivity. This spectrum helps to visualize the possible frequency notches caused by this example.

Then, zero offset simulation with and without multiples were made. Simulations were done using the algorithm proposed by Mendel et al. (1979). Figure (4) portrays the input reflectivity model and the output impulse Response for the Ricker wavelet traveling through such reflectivity. From figure (5) illustrates the O'Doherty and Anstey theoretical amplitude spectrum and the computed spectrum for the transmitted signal. Based on the theoretical amplitude spectrum it should be expected to find a drop in the amplitude between 50 Hz up to 90 Hz. The computed periodogram for the zero offset data corroborates this lack of frequency content in a window between 0.5-0.7 sec.
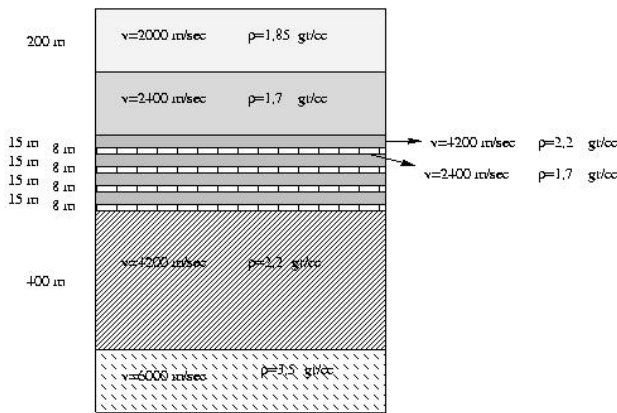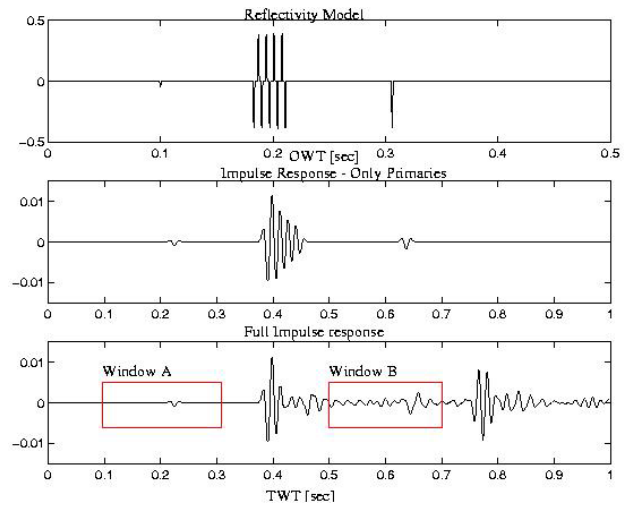

Figure 4: Top: reflectivity model. Middle: zero offset-impulse response (only primaries). Bottom: zero offset-full response. Window A stands for 'Above the transmission filter' and B stands for 'Below the transmission filter'.

Figure 3: Earth model for a transmision filter

A simulation with offset was also performed by means of the reflectivity method (Kennet, 1983).

Shot gather data corroborates the drop in the amplitude spectrum observed for the same reflectivity model at zero offset simulations. It is interesting to note that, as observed by Perz (2000), the effect of the transmission filter does not seem to have a strong dependency on offset (figure 7).

Next, the normal moveout correction (NMO) was applied and data was stacked to minimize the effect of multiples. However, since we are working beyond the limits of resolution there are still some remnants of multiple energy in the stack section. Notice that the arrival below the transmission filter is delayed by almost 90 degrees, being
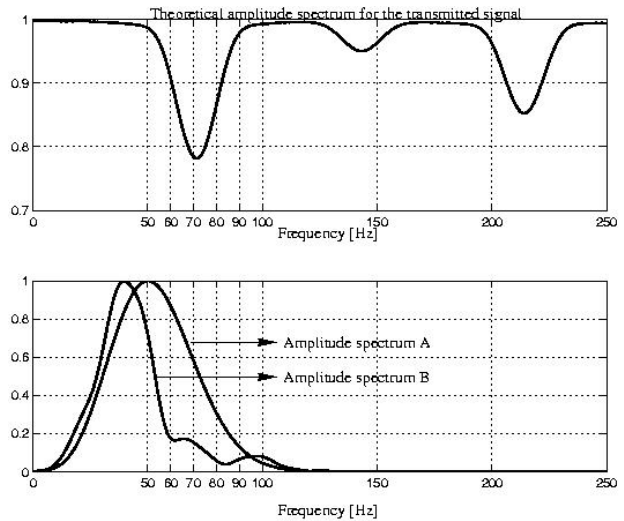

Figure 5: O'Doherty and Anstey theoretical amplitude spectrum for the transmitted signal. Bottom: amplitude spectrum A for data between 0.1-0.3 sec overlying amplitude spectrum B for data between 0.5-0.7 sec.

a trough instead of a peak at t=0.612 sec. This effect on the phase of the signal was pointed out by Banik (1985b), Coulombe and Bird (1996) and by Perz (2000).
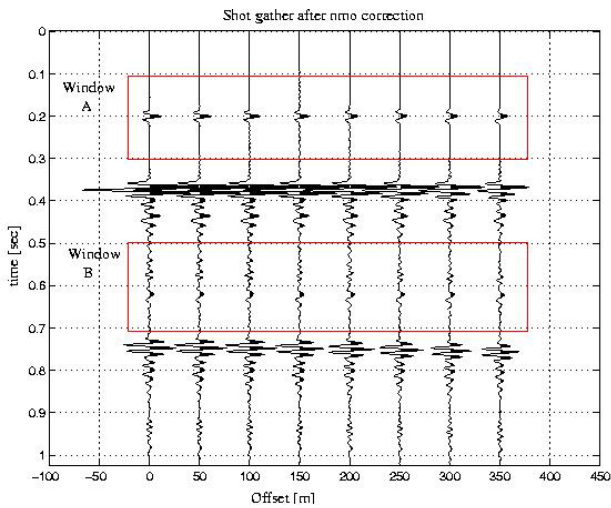
Figure 6: Full impulse response with offset. Window A stands for 'Above the transmission filter' and B stands for 'Below the transmission filter'.
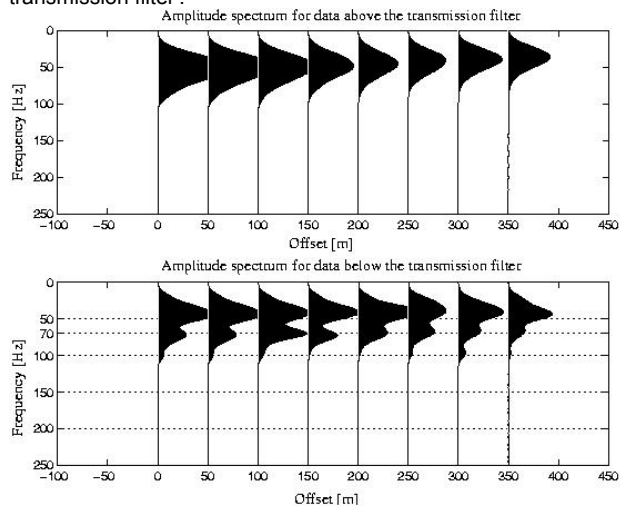

Figure 7: Top: amplitude spectrum for data between 0.1-0.3 sec. Bottom: amplitude spectrum for data between 0.5-0.7 sec, below transmission filter.
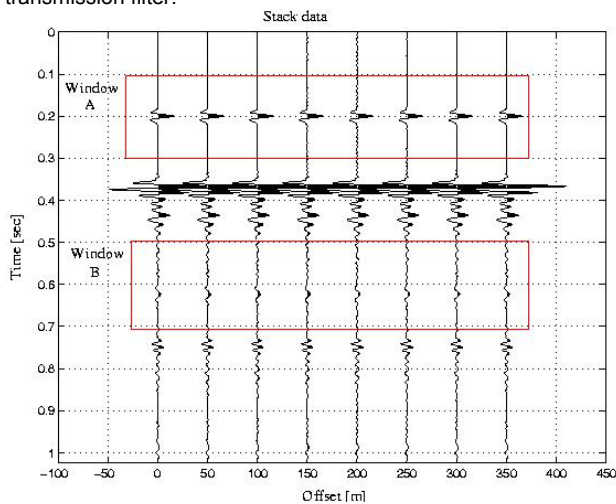

Figure 8: Full impulse response-stack data. Window A stands for 'Above the transmission filter' and B stands for 'Below the transmission filter'. Stacked trace was repeated for plotting purposes.

This example is intended to illustrate our technique proposed to compensate for the effect of the transmission filter. A window above the transmission filter was chosen between 0.1-0.3 sec (window A). Another window below the transmission filter was chosen between 0.5-0.7 sec (window B). Data and the amplitude spectrum for these windows are shown in figure (9).

We define the transfer function TRF(ω) in the frequency domain as the one computed by dividing the spectra from window A and window B in the frequency range between 25-75 Hz.
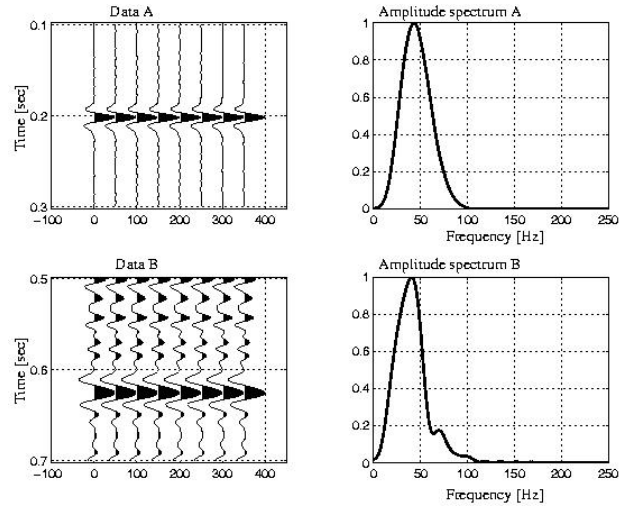

Figure 9: Top left: data A (Above transmission filter). Top right: amplitude spectrum A for data A. Bottom left: data B (Below transmission filter). Bottom right: amplitude spectrum B for data B.

Using conventional deconvolution, the corresponding wavelets above and below the transmission filter were extracted. Figures (10) and (11) present the extracted wavelet for each case with their corresponding amplitude spectrum. It can be seen from them that the amplitude spectrum of the wavelet below the transmission filter is shifted toward the low frequencies.
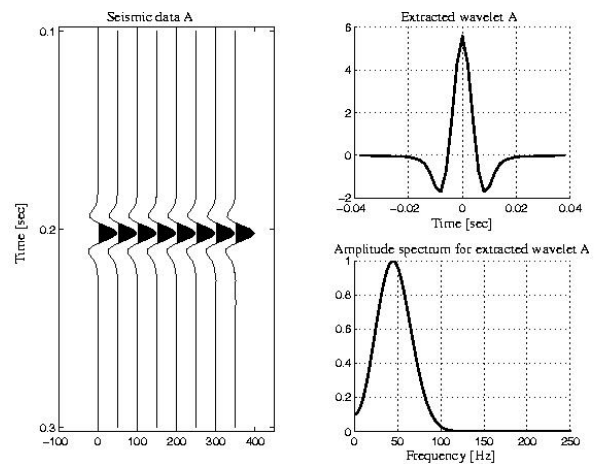

Figure 10: Right: data A (Above transmission filter). Left top: extracted wavelet from data A by conventional deconvolution. Left bottom: amplitude spectrum of extracted wavelet A.
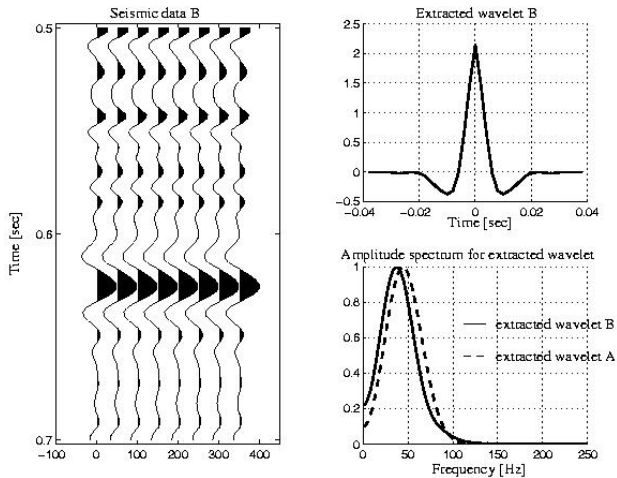
Figure 11: Right: data B (Below transmission filter). Left top: extracted wavelet from data B by conventional deconvolution. Left bottom: amplitude spectrum of extracted wavelet B overlying amplitude spectrum of extracted wavelet A.

Next, the transfer filter $trf_{min}(t)$ was computed and convolved with the data below the transmission filter. Figure (12) compared data below transmission filter before and after applying the compensatory filter. It can be seen an increment in frequency content after filtered and also notice that the signal was slightly correct in terms of phase. In terms of the amplitude spectrum of the signal below the transmission filter, after convolution with $trf_{min}(t)$, it was possible to boost up the spectrum at the notch window. However, the result overestimates the amplitude for frequencies towards the end of the spectrum (figure 13).
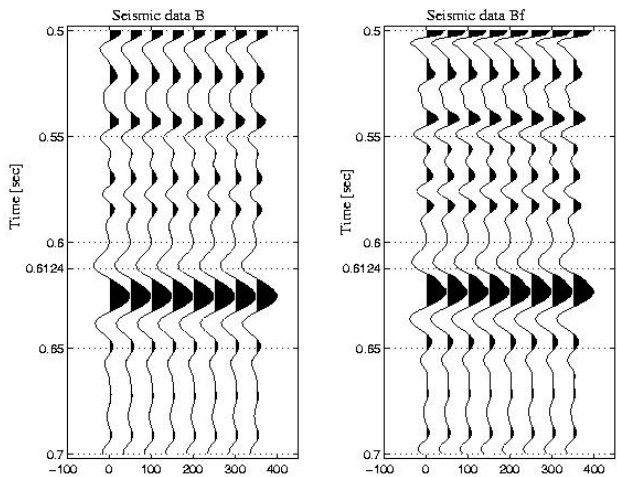

Figure 12: Left: seismic data B, Below transmission filter. Right: seismic data Bf, Below transmission Filter after applying compensatory filter to overcome the loss in frequency content trf_{min} (equation 3).

Finally, conventional deconvolution was applied to extract the corresponding wavelet from the data below the transmission filter after compensatory filtering (figure 14)
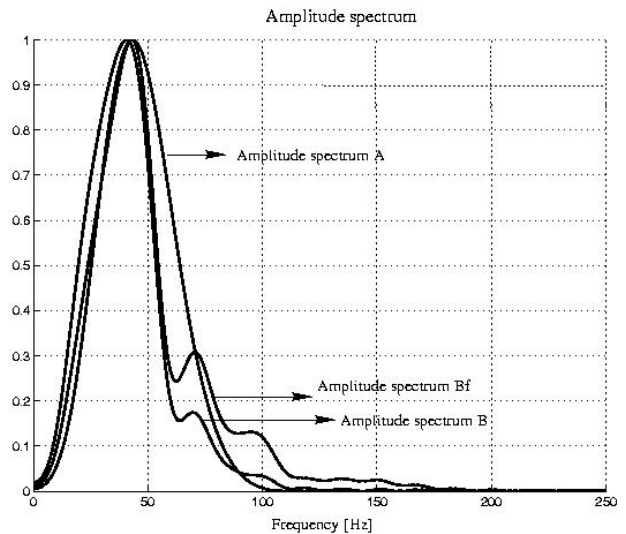

Figure 13: Amplitude spectrum A for the data above the transmission filter, overlying the amplitude spectrum B for data below the transmission filter and amplitude spectrum Bf for data below transmission filter after applying compensatory filter trf_{min}
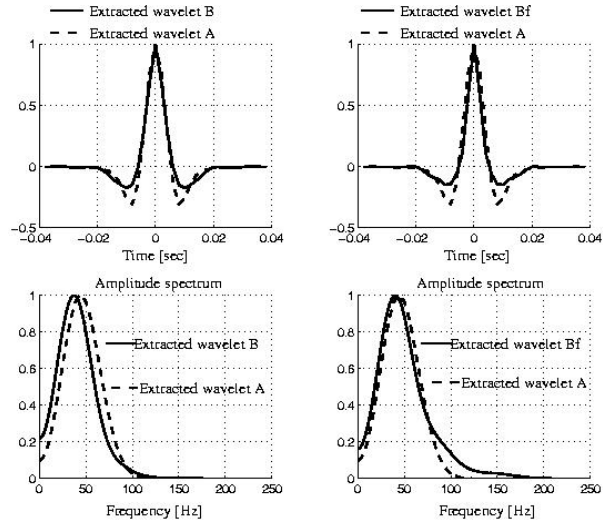

Figure 14: Top left: extrated wavelet B from data below the transmission filter. Bottom left: amplitude spectrum of the extracted wavelet B overlying amplitude spectrum from extracted wavelet A (Above transmission filter). Top right:extrated wavelet Bf from data below the transmission filter, after compensatory filter. Bottom right: amplitude spectrum of the extracted wavelet Bf, overlying amplitude spectrum from extracted wavelet A.

The amplitude spectrum of the filtered wavelet seems to be a better approximation for the extracted wavelet above the transmission filter.

Summary and Conclusions

The approach proposed to overcome the effect of stratigraphic filtering is easy to implement and able to improve the signal below the stratigraphic filter. It is recommended to apply this technique after stack to minimize multiple contribution. Our examples illustrate the apparent attenuation due to stratigraphic layering. The computed amplitude spectrum for the signal below the

transmission filter corroborates the predicted notches from the theoretical amplitude spectrum given by O'Doherty and Anstey.

Data below the transmission filter was convolved with the compensatory filter and afterward conventional deconvolution was used for wavelet extraction. Comparisons between extracted wavelets below the transmission filter before and after applying the compensatory filter show the effectiveness of the applied compensation. The extracted wavelet and its amplitude spectrum below transmission filter after compensatory filter resembles better the wavelet above transmission filter.

So far, the existent literature on this subject propose to include a post stack two gate deconvolution (gate above and below the transmission filter) to remove the effects caused by the presence of coals (Coulombe and Bird, 1996). The approach presented in this paper is easy to implement and could be a way to normalize the wavelet along the seismogram.

Acknowledgments

References

Banik, N., Lerche, I., Resnick, J. R., and Shuey, R. T., 1985a, Stratigraphic filtering, part II: Model spectra: Geophysics, 50, 2775-2783.

___1985b, Stratigraphic filtering, part I: Derivation of the O'Doherty-Anstey formula: Geophysics, 50, 2768-2774.

Claerbout, J. F., 1976, Fundamentals of Geophysical data processing: New York, McGraw-Hill Book Co. Inc.

Coulombe, C., and Bird, D. N., 1996, Transmission filtering by high-amplitude reflection coefficients: theory, practice and processing considerations: The Leading Edge, 15, 1037-1042.

Kennet, N., 1983, Seismic wave propagation in stratified media: Cambridge University Press.

Mendel, N., and Chan, 1979, Synthetic seismograms using the state-space approach: Geophysics, 44, 880-895.

O'Doherty and Anstey, 1971, Reflections on amplitudes: Geophysical Prospecting, 19,430-458.

Perz, M., 2000, Angle-dependent coal transmission filtering in the Western Canadian Basin: a numerical study: SEG 2000 Expanded Abstracts, 12, 2020-2023.

Schoenberger, M., and Levin, F. K., 1974, Apparent attenuation due to intrabed multiples : Geophysics, 39, 278-291.

Widess, M., 1973, How thin is a thin bed?: Geophysics, 38, 1176-1180.

Yilmaz, 1987, Seismic data processing: Society of Exploration Geophysicists.